Model Order Reductions for Stability Analysis of Islanded Microgrids With Droop Control

Mariani, Valerio; Vasca, Francesco; Vásquez, Juan C.; Guerrero, Josep M.

Published in:
I E E E Transactions on Industrial Electronics

DOI (link to publication from Publisher):
10.1109/TIE.2014.2381151

Publication date:
2015

Document Version
Early version, also known as pre-print

Model Order Reductions for Stability Analysis of Islanded Microgrids with Droop Control

V. Mariani, F. Vasca, *Senior Member, IEEE*,
J. C. Vásquez, *Member, IEEE* and J. M. Guerrero, *Senior Member, IEEE*

***Abstract*—Three-phase inverters subject to droop control are widely used in islanded microgrids to interface distributed energy resources to the network and to properly share the loads among different units. In this paper, a mathematical model for islanded microgrids with linear loads and inverters under frequency and voltage droop control is proposed. The model is constructed by introducing a suitable state space transformation which allows to write the closed loop model in an explicit state space form. Then, the singular perturbations technique is used to obtain reduced order models which reproduce the stability properties of the original closed loop model. The analysis shows that the currents dynamics influence the stability of the microgrid particularly for high values of the frequency droop control parameters. It is also shown that a further reduction of the model order leads to the typical oscillator model which is not able to predict the possible instability of the droop controlled system. Numerical and experimental results demonstrate the validity of the proposed models.**

***Index Terms*—Droop control, microgrids, power systems stability, power systems modeling.**

I. Introduction

Microgrids consist of interconnected distributed storages and energy resources that supply for local loads power demand. Typically, the energy resources are interfaced to the network via suitably controlled inverters. A widely used control technique for the distributed energy resources inverters is the droop control, which was initially proposed in [1] to mimic synchronous generators. The droop control allows to properly support the power demands without communication among the inverters [2], [3], [4]. This control technique has been also adapted in order to fit scenarios such as non inductive line impedances [5], [6], dynamic and nonlinear loads [7], [8], [9], unbalances [10], [11], [12], transitions between islanded and grid-connected modes [13], [14], [15]. Specific solutions in order to mitigate some drawbacks such as the slow transient response [16], [17] and the inherent trade-off between power sharing capabilities and frequency/voltage regulation [18], [19] have been also proposed. A hierarchical design and a nonlinear outer control loop to overcome some issues related to droop controlled inverters in microgrids are proposed in [20] and [21], respectively.

The nonlinearity of the droop control laws makes the determination of a closed loop model a nontrivial task, even in presence of few inverters and linear loads. On the other hand, an accurate model is crucial for a precise and rigorous assessment of the microgrid stability. Different approaches and techniques have been proposed in the literature to model microgrids with droop controlled inverters. In [21], [22], [23], the electric passive network is represented as an interconnection of impedances at the nominal frequency. The stability of the corresponding closed loop small-signal models does not depend on the droop control parameters. In other papers, either by means of dynamic phasors [24], [25], [26] or by taking into account relevant dynamics according to specific scenarios [27], [28], the closed loop model of the microgrid is shown to be unstable for large droop control parameters. In [29] and [30] the stability analysis of droop controlled inverters is approached via contraction theory. In [31] the stability condition is formulated as a synchronization problem of generalized Kuramoto oscillators. According to this framework, the stable equilibrium point of the system is achieved when all the microgrid inverters generate voltages with the same frequency. The model in [31] does not consider the dynamic equations of loads and currents. On the other hand, in some situations such dynamics become prominent and can strongly affect the stability of the microgrid [32], [33]. In particular, the small-signal models analyzed in [34] clearly highlight the presence of unstable behaviors for large values of the droop parameters.

In this paper, a systematic approach for the construction of a dynamic model of three-phase AC microgrids with inverters under classical voltage and frequency droop controls is presented. The adoption of a state space transformation based on "local" rotation matrices allows to write the model in a state space explicit form which also includes the line and loads dynamics. Differently from [34], the rotation matrices used for the proposed state transformation do not have a common reference frame and are directly applied to the nonlinear large signal model. Moreover the proposed model does not consider the powers filters neither the filters at the output of the inverters, which is an intriguing assumption because it makes more complex the derivation of the closed loop equations. Indeed algebraic loops are present because the powers used in the droop controller are not considered as state variables. The model shows the presence of unstable equilibrium points for large values of the frequency droop control parameter.

Manuscript received May 27, 2014. Accepted for publication November 7, 2014.

V. Mariani and F. Vasca are with the Department of Engineering, University of Sannio, Piazza Roma 21, 82100 Benevento, Italy (email: valerio.mariani@unisannio.it, francesco.vasca@unisannio.it)

J. C. Vásquez and J. M. Guerrero are with the Department of Energy Technology, Pontoppidanstræde 101, Aalborg University, Aalborg, Denmark (email: juq@et.aau.dk, joz@et.aau.dk)

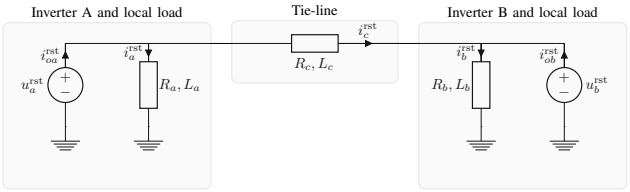

Fig. 1. AC microgrid in islanded-mode with two inverters and two local loads. The superscripts r, s and t refer to a three-phase balanced system.

By using the singular perturbations technique, reduced order models at different time scales are derived and it is shown that their stability reproduce that of the original closed loop model.

The rest of the paper is organized as follows. In Sec. II a closed loop model of a three-phase AC microgrid consisting of two inverters under frequency and voltage droop controls, a resistive-inductive tie-line and two local resistive-inductive loads is derived. In Sec. III, by applying the singular perturbations technique, reduced order models corresponding to different dominant time-constants are obtained. It is also shown that the proposed reduced order models can be veiwed as a generalization of the classical Kuramoto oscillator model. In Sec. IV, numerical simulations show that the reduced order models are able to estimate the droop control parameters for which the corresponding full order model is unstable while, on the contrary, the model with Kuramoto oscillators is always stable. In Sec. V experimental results on a real microgrid validate the proposed models and confirm the possible existence of unstable behaviors. Sec. VI concludes the paper.

II. Microgrid Model Under Droop Control

An equivalent circuit of the three-phase AC microgrid under investigation is depicted in Fig. 1. Two inverters and their corresponding balanced resistive-inductive local loads, with resistances R_a, R_b and inductances L_a, L_b, respectively, are connected through a balanced resistive-inductive tie-line with resistance R_c and inductance L_c. A wide class of more complex linear topologies of microgrids can be recasted in the equivalent structure shown in Fig. 1 by using standard ciruit theory transformations.

A. Open Loop Model

Assume each inverter is represented by a three-phase ideal voltage source generating a symmetric direct voltage sequence. By applying the Kirchhoff voltage laws to the equivalent circuit depicted in Fig. 1 and by representing voltages and currents in a stationary reference frame indicated with superscripts α and β, one obtains

$$L_k \frac{d}{dt} i_k^{\alpha\beta} = - R_k i_k^{\alpha\beta} + u_k^{\alpha\beta}, \qquad k = a, b \tag{1a}$$

$$L_c \frac{d}{dt} i_c^{\alpha\beta} = - R_c i_c^{\alpha\beta} + u_a^{\alpha\beta} - u_b^{\alpha\beta}, \tag{1b}$$

where the index k denotes the inverter and

$$u_k^{\alpha\beta} = \begin{pmatrix} u_k^{\alpha} & u_k^{\beta} \end{pmatrix}^{\top}, \qquad k = a, b, \tag{2a}$$

$$i_k^{\alpha\beta} = \begin{pmatrix} i_k^{\alpha} & i_k^{\beta} \end{pmatrix}^{\top}, \qquad k = a, b, \tag{2b}$$

$$i_c^{\alpha\beta} = \begin{pmatrix} i_c^{\alpha} & i_c^{\beta} \end{pmatrix}^{\top}, \tag{2c}$$

$$i_{ok}^{\alpha\beta} = \begin{pmatrix} i_{ok}^{\alpha} & i_{ok}^{\beta} \end{pmatrix}^{\top}, \qquad k = a, b, \tag{2d}$$

are the vectors of inverters voltages (inputs), local loads currents (state variables), line currents (state variables) and inverters currents, respectively. The state space equations (1) correspond to a sixth order dynamic model. The model (1) is usually rewritten in a rotating reference frame synchronous with the common nominal frequency, say ω. Instead, in this paper a different rotation matrix for each current vector is considered. In particular, the following state space transformation is defined

$$\begin{pmatrix} i_a^{\mathrm{dq}} \\ i_b^{\mathrm{dq}} \\ i_c^{\mathrm{dq}} \end{pmatrix} = \begin{pmatrix} \Gamma(\theta_a)^{-1} & 0 & 0 \\ 0 & \Gamma(\theta_b)^{-1} & 0 \\ 0 & 0 & \Gamma(\theta_a)^{-1} \end{pmatrix} \begin{pmatrix} i_a^{\alpha\beta} \\ i_b^{\alpha\beta} \\ i_c^{\alpha\beta} \end{pmatrix}, \tag{3}$$

where the superscripts d and q denote variables in rotating reference frames, the rotation matrices are given by

$$\Gamma(\theta_k) = \begin{pmatrix} \cos\theta_k & -\sin\theta_k \\ \sin\theta_k & \cos\theta_k \end{pmatrix}, \qquad k = a, b, \tag{4}$$

and θ_k is the angle that in the closed loop model will be determined by the droop control of the k-th inverter. The choice (3)-(4) is similar to the transformation considered in [34], but for the proposed model no common reference frame is considered which allows to "decouple" for each inverter the active and reactive powers expressions with respect to the corresponding currents components, so as it is shown in next Subsection. Note that the current $i_c^{\alpha\beta}$ is transformed by using the rotation matrix of the inverter a (or analogously one can choose the angle of the inverter b). By using (4) one can write

$$\Gamma(\theta_k)^{-1} \frac{d}{dt} \Gamma(\theta_k) = \begin{pmatrix} 0 & -1 \\ 1 & 0 \end{pmatrix} \frac{d}{dt} \theta_k = \Omega \frac{d}{dt} \theta_k, \tag{5}$$

with

$$\Omega = \begin{pmatrix} 0 & -1 \\ 1 & 0 \end{pmatrix}. \tag{6}$$

Moreover, from (4) it follows that

$$\Gamma(\delta)^{-1} = \Gamma(\theta_a)^{-1} \Gamma(\theta_b), \tag{7}$$

where $\delta = \theta_a - \theta_b$. By applying (3) to (1) and by using (5)-(7) one obtains

$$L_k \frac{d}{dt} i_k^{\mathrm{dq}} = - R_k i_k^{\mathrm{dq}} - L_k \Omega \frac{d}{dt} \theta_k \, i_k^{\mathrm{dq}} + u_k^{\mathrm{dq}}, \quad k = a, b, \tag{8a}$$

$$L_c \frac{d}{dt} i_c^{\mathrm{dq}} = - R_c i_c^{\mathrm{dq}} - L_c \Omega \frac{d}{dt} \theta_a \, i_c^{\mathrm{dq}} + u_a^{\mathrm{dq}} - \Gamma(\delta)^{-1} u_b^{\mathrm{dq}}. \tag{8b}$$

The state variables of the open loop model (8) are the local loads currents i_k^{dq} and the line currents i_c^{dq}, while the inputs are the inverters voltages u_k^{dq} and the angles θ_k. The choice

of the rotating reference frame synchronous with the voltage generated by each inverter implies that

$$u_k^{\rm dq} = \begin{pmatrix} u_k^d & u_k^q \end{pmatrix}^\top = \begin{pmatrix} U_k & 0 \end{pmatrix}^\top, \qquad k = a, b. \tag{9}$$

The condition (9) will be exploited in order to obtain an explicit state space form of the closed loop dynamic model under droop control. It is important to stress that the construction of the model (8) does not imply any apriori synchronization assumption of the two inverters.

The "local" frequencies $(d/dt)\theta_k$ and amplitudes U_k in (8)-(9) are determined by the controllers which implement the frequency and voltage droop laws

$$\frac{d}{dt}\theta_k = \omega + m_k(\bar{P}_k - P_k), \qquad k = a, b, \tag{10a}$$

$$U_k = \bar{U}_k + n_k(\bar{Q}_k - Q_k), \qquad k = a, b, \tag{10b}$$

where ω is the nominal frequency, $\bar{U}_k$ are the voltage references, m_k and n_k are the frequency and voltage droop coefficients, $\bar{P}_k$ and $\bar{Q}_k$ are the active and reactive power references, P_k and Q_k are the active and reactive powers. The closed loop model will be obtained by expressing the powers as functions of the microgrid state variables.

Notice that the active and reactive powers are invariant under rotations, therefore, the choice of the synchronous reference frames defined by (3)-(4) does not affect the particular implementation of the droop controllers (10) in a real system. Moreover, the two initial conditions of (10a) are independent.

B. Closed Loop Model

In order to derive a closed loop model from (8)-(10), the powers P_k and Q_k must be expressed in terms of the variables $i_a^{\rm dq}$, $i_b^{\rm dq}$, $i_c^{\rm dq}$ and δ. To this aim define

$$\Gamma_k(\delta) = \begin{cases} I & k = a, \\ -\Gamma(\delta) & k = b, \end{cases} \tag{11}$$

where I is the identity matrix of suitable dimensions. Then, by using (9) one can write

$$P_k = (u_k^{\alpha\beta})^\top \, i_{ok}^{\alpha\beta} = (u_k^{\rm dq})^\top \, i_{ok}^{\rm dq} = U_k i_{ok}^d, \qquad k = a, b, \tag{12a}$$

$$Q_k = (u_k^{\alpha\beta})^\top \Omega \, i_{ok}^{\alpha\beta} = (u_k^{\rm dq})^\top \Omega \, i_{ok}^{\rm dq} = -U_k i_{ok}^q, \quad k = a, b, \tag{12b}$$

where the inverters currents in the rotating reference frames can be expressed as

$$i_{ok}^{\rm dq} = \Gamma(\theta_k)^{-1} i_{ok}^{\alpha\beta}, \qquad k = a, b. \tag{13}$$

The voltages U_k can be explicitly expressed in terms of the inverters currents i_{ok}^q by combining (12b) and (10b). By solving the corresponding algebraic loop one obtains

$$U_k = \frac{\bar{U}_k + n_k \bar{Q}_k}{1 - n_k \, i_{ok}^q}, \quad k = a, b, \tag{14}$$

From (14) it is clear that in order to obtain the closed loop model in explicit state space form one needs to express the inverters currents $i_{ok}^{\rm dq}$, with $k = a, b$, in terms of the state variables $i_a^{\rm dq}$, $i_b^{\rm dq}$, $i_c^{\rm dq}$ and δ. By applying the Kirchhoff current laws to the circuit in Fig. 1 one can write

$$i_{oa}^{\alpha\beta} = i_a^{\alpha\beta} + i_c^{\alpha\beta}, \tag{15a}$$

$$i_{ob}^{\alpha\beta} = i_b^{\alpha\beta} - i_c^{\alpha\beta}. \tag{15b}$$

By using (13) and (15), together with the inverse of (3), with simple algebraic manipulations one obtains

$$i_{ok}^{\rm dq} = i_k^{\rm dq} + \Gamma_k(\delta) i_c^{\rm dq}, \qquad k = a, b, \tag{16}$$

where $\Gamma_k(\delta)$ are defined in (11). By substituting (12) and (14) in (8)-(10), the closed loop model of the microgrid under droop control can be written as

$$\begin{aligned} \frac{L_k}{R_k}\frac{d}{dt} i_k^{\rm dq} = &- \left(I + \frac{X_k}{R_k}\Omega \right) i_k^{\rm dq} \\ &- \frac{L_k}{R_k}\Omega m_k \left(\bar{P}_k - \frac{\bar{U}_k + n_k \bar{Q}_k}{1 - n_k i_{ok}^q} i_{ok}^d \right) i_k^{\rm dq} \\ &+ \frac{1}{R_k} \frac{\bar{U}_k + n_k \bar{Q}_k}{1 - n_k i_{ok}^q} \begin{pmatrix} 1 \\ 0 \end{pmatrix}, \quad k = a, b, \end{aligned} \tag{17a}$$

$$\begin{aligned} \frac{L_c}{R_c}\frac{d}{dt} i_c^{\rm dq} = &- \left(I + \frac{X_c}{R_c}\Omega \right) i_c^{\rm dq} \\ &- \frac{L_c}{R_c}\Omega m_a \left(\bar{P}_a - \frac{\bar{U}_a + n_a \bar{Q}_a}{1 - n_a i_{ok}^q} i_{ok}^d \right) i_c^{\rm dq} \\ &+ \frac{1}{R_c} \sum_{j=a,b} \Gamma_j(\delta)^{-1} \frac{\bar{U}_j + n_j \bar{Q}_j}{1 - n_j i_{oj}^q} \begin{pmatrix} 1 \\ 0 \end{pmatrix}, \end{aligned} \tag{17b}$$

$$\begin{aligned} \frac{d}{dt}\delta = &\, m_a \left(\bar{P}_a - \frac{\bar{U}_a + n_a \bar{Q}_a}{1 - n_a i_{oa}^q} i_{oa}^d \right) \\ &- m_b \left(\bar{P}_b - \frac{\bar{U}_b + n_b \bar{Q}_b}{1 - n_b i_{ob}^q} i_{ob}^d \right). \end{aligned} \tag{17c}$$

The closed loop model (16)-(17) is a seventh order system with state variables $i_k^{\rm dq}$, $i_c^{\rm dq}$ and δ with $k = a, b$. Note that the output currents $i_{ok}^{\rm dq}$ depend on all seven state variables through (16), which makes the closed loop model rather complex.

III. Reduced Order Models

The simple microgrid topology considered in this paper can be viewed as a basic subsystem of more complex microgrids. Then, It is interesting to consider possible simplifications of the closed loop model (16)-(17), provided that the stability properties are not lost due to the model order reductions. In this Section, by using the singular perturbations technique [35], reduced order models which exploit different dominant time-constants are obtained.

A. Dominant Loads Time-Constants

For many microgrids the tie-line time-constant L_c/R_c is much smaller than the loads time-constants L_a/R_a and L_b/R_b [36]. Assume that the conditions

$$\frac{L_c}{R_c} \ll \frac{L_k}{R_k}, \qquad k = a, b, \tag{18}$$

hold. In order to obtain the reduced order model one can set L_c/R_c to zero in (17b). The practical values for the grid electrical parameters and frequency ω justify the fact that

X_c/R_c is not assumed to be zero. Then, indicate with z the variables (currents) solving the equations obtained with the singular perturbations approach. By expressing (16) in terms of the corresponding variables of the reduced order model it follows

$$z_{ok}^{\mathrm{dq}} = z_k^{\mathrm{dq}} + \Gamma_k(\delta_z) z_c^{\mathrm{dq}}, \tag{19}$$

and from (17b) one obtains

$$\begin{aligned} 0 =& -\left(I + \frac{X_c}{R_c}\Omega\right)\Gamma_k(\delta_z)^{-1}(z_{ok}^{\mathrm{dq}} - z_k^{\mathrm{dq}}) \\ &+ \frac{1}{R_c}\sum_{j=a,b}\Gamma_j(\delta_z)^{-1}\frac{\bar{U}_j + n_j\bar{Q}_j}{1 - n_j\, z_{oj}^q}\begin{pmatrix}1\\0\end{pmatrix}, \quad k = a, b. \end{aligned} \tag{20}$$

where δ_z is the angle corresponding to the reduced order model. The four scalar equations (20) are quadratic algebraic constraints that relate z_{ok}^{dq} to z_k^{dq}. It is simple to verify that for each k there exists a unique solution of (20) for z_{ok}^{dq} with positive inverter voltage amplitude. Then (20) can be interpreted as a unique mapping from z_k^{dq} to z_{ok}^{dq}.

The reduced order model with singular perturbations can be now directly obtained from (17a) and (17c):

$$\begin{aligned} \frac{L_k}{R_k}\frac{d}{dt}z_k^{\mathrm{dq}} =& -\left(I + \frac{X_k}{R_k}\Omega\right) z_k^{\mathrm{dq}} \\ &- \frac{L_k}{R_k}\Omega m_k\left(\bar{P}_k - \frac{\bar{U}_k + n_k\bar{Q}_k}{1 - n_k\, z_{ok}^q} z_{ok}^d\right) z_k^{\mathrm{dq}} \\ &+ \frac{1}{R_k}\frac{\bar{U}_k + n_k\bar{Q}_k}{1 - n_k\, z_{ok}^q}\begin{pmatrix}1\\0\end{pmatrix}, \qquad k = a, b, \end{aligned} \tag{21a}$$

$$\begin{aligned} \frac{d}{dt}\delta_z =& m_a\left(\bar{P}_a - \frac{\bar{U}_a + n_a\bar{Q}_a}{1 - n_a\, z_{oa}^q} z_{oa}^d\right) \\ &- m_b\left(\bar{P}_b - \frac{\bar{U}_b + n_b\bar{Q}_b}{1 - n_b\, z_{ob}^q} z_{ob}^d\right), \end{aligned} \tag{21b}$$

where z_{ok}^{dq}, with $k = a, b$, can be written as functions of the five state variables z_k^{dq} and δ_z by using (20). In next Section the fifth order model (20)-(21) will be shown to be able to estimate the interval of m_k for which the seventh order model (16)-(17) is unstable. It should be noticed that the reduced order model (20)-(21) under (18) is not equivalent to the model which can be obtained from (16)-(17) by assuming the currents i_c^{dq} to be at steady-state. Indeed (20) is more simple than (17b) at steady-state.

B. Dominant Tie-Line Time-Constants

A different reduced order model can be obtained if the tie-line time-constant is much greater than the load time-constants. Assume that the conditions

$$\frac{L_k}{R_k} \ll \frac{L_c}{R_c}, \qquad k = a, b, \tag{22}$$

hold. In order to obtain the reduced order model set L_k/R_k to zero in (17a). The practical values for the grid electrical parameters and frequency ω justify the fact that X_k/R_k is not assumed to be zero. Then, indicate with ζ the variables obtained from the currents with the singular perturbations approach. By expressing (16) in terms of the corresponding variables of the reduced order model it follows

$$\zeta_{ok}^{\mathrm{dq}} = \zeta_k^{\mathrm{dq}} + \Gamma_k(\delta_\zeta)^{-1}\zeta_c^{\mathrm{dq}}, \tag{23}$$

and from (17a) one obtains

$$\begin{aligned} 0 =& -\left(I + \frac{X_k}{R_k}\Omega\right)(\zeta_{ok}^{\mathrm{dq}} - \Gamma_k(\delta_\zeta)^{-1}\zeta_c^{\mathrm{dq}}) \\ &+ \frac{1}{R_k}\frac{\bar{U}_k + n_k\bar{Q}_k}{1 - n_k\,\zeta_{ok}^q}\begin{pmatrix}1\\0\end{pmatrix}, \qquad k = a, b, \end{aligned} \tag{24}$$

where δ_ζ is the variable in the reduced order model corresponding to the angle difference δ. The equations (24) are four scalar quadratic algebraic constraints that relate ζ_{ok}^{dq} to the three state variables ζ_c^{dq} and δ_ζ. It is simple to verify that for each k there exists a unique solution of (24) for ζ_{ok}^{dq} with positive inverter voltage amplitude. Then (24) can be interpreted as a unique mapping from the state variables to ζ_{ok}^{dq}.

The reduced order model with singular perturbations can be now directly obtained from (17b) and (17c):

$$\begin{aligned} \frac{L_c}{R_c}\frac{d}{dt}\zeta_c^{\mathrm{dq}} =& -\left(I + \frac{X_c}{R_c}\Omega\right)\zeta_c^{\mathrm{dq}} \\ &- \frac{L_c}{R_c}\Omega m_a\left(\bar{P}_a - \frac{\bar{U}_a + n_a\bar{Q}_a}{1 - n_a\,\zeta_{oa}^q}\zeta_{oa}^d\right)\zeta_c^{\mathrm{dq}} \\ &+ \frac{1}{R_c}\sum_{j=a,b}\Gamma_j(\delta_\zeta)^{-1}\frac{\bar{U}_j + n_j\bar{Q}_j}{1 - n_j\,\zeta_{oj}^q}\begin{pmatrix}1\\0\end{pmatrix}, \end{aligned} \tag{25a}$$

$$\begin{aligned} \frac{d}{dt}\delta_\zeta =& m_a\left(\bar{P}_a - \frac{\bar{U}_a + n_a\bar{Q}_a}{1 - n_a\,\zeta_{oa}^q}\zeta_{oa}^d\right) \\ &- m_b\left(\bar{P}_b - \frac{\bar{U}_b + n_b\bar{Q}_b}{1 - n_b\,\zeta_{ob}^q}\zeta_{ob}^d\right), \end{aligned} \tag{25b}$$

where ζ_{ok}^{dq} can be written as a function of the state variables ζ_c^{dq} and δ_ζ by using (24).

The third order model (24)-(25) will be shown, in next Section, to be able to predict unstable behaviors for some values of m_k for which the seventh order model (16)-(17) is unstable under (22).

C. Reduced Order Models without Voltage Droop

In many microgrids, the inverters are subject only to the frequency component of the droop control because there is no reactive power demand to be satisfied. In the case of dominant loads microgrids a reduced order model for this type of closed loop system can be derived by setting $n_a = 0$ and $n_b = 0$ in (20)-(21), which leads to

$$\begin{aligned} z_{ok}^{\mathrm{dq}} =& z_k^{\mathrm{dq}} + \frac{1}{R_c}\Gamma_k(\delta_z)\left(I + \frac{X_c}{R_c}\Omega\right)^{-1} \\ &\cdot \sum_{j=a,b}\Gamma_j(\delta_z)^{-1}\bar{U}_j\begin{pmatrix}1\\0\end{pmatrix}, \quad k = a, b, \end{aligned} \tag{26}$$

and

$$\frac{L_k}{R_k}\frac{d}{dt}z_k^{\mathrm{dq}} = -\left(I+\frac{X_k}{R_k}\Omega\right)z_k^{\mathrm{dq}} - \frac{L_k}{R_k}\Omega m_k\left(\bar{P}_k-\bar{U}_k z_{ok}^d\right)z_k^{\mathrm{dq}} + \frac{\bar{U}_k}{R_k}\begin{pmatrix}1\\0\end{pmatrix}, \qquad k=a,b, \tag{27a}$$

$$\frac{d}{dt}\delta_z = m_a\left(\bar{P}_a-\bar{U}_a z_{oa}^d\right) - m_b\left(\bar{P}_b-\bar{U}_b z_{ob}^d\right). \tag{27b}$$

In the case of dominant line microgrids it is possible to operate similar considerations in order to obtain a corresponding reduced order model. Particularly, set $n_a = 0$ and $n_b = 0$ in (24)-(25). Then, it follows

$$\zeta_{ok}^{\mathrm{dq}} = \Gamma_k(\delta_\zeta)^{-1}\zeta_c^{\mathrm{dq}} + \frac{1}{R_k}\left(I+\frac{X_k}{R_k}\Omega\right)^{-1}\bar{U}_k\begin{pmatrix}1\\0\end{pmatrix}, \quad k=a,b, \tag{28}$$

and

$$\frac{L_c}{R_c}\frac{d}{dt}\zeta_c^{\mathrm{dq}} = -\left(I+\frac{X_c}{R_c}\Omega\right)\zeta_c^{\mathrm{dq}} - \frac{L_c}{R_c}\Omega m_a\left(\bar{P}_a-\bar{U}_a\zeta_{oa}^d\right)\zeta_c^{\mathrm{dq}} + \frac{1}{R_c}\sum_{j=a,b}\Gamma_j(\delta_\zeta)^{-1}\bar{U}_j\begin{pmatrix}1\\0\end{pmatrix}, \tag{29a}$$

$$\frac{d}{dt}\delta_\zeta = m_a\left(\bar{P}_a-\bar{U}_a\zeta_{oa}^d\right) - m_b\left(\bar{P}_b-\bar{U}_b\zeta_{ob}^d\right). \tag{29b}$$

The numerical analysis in next Section will show the influence of the frequency droop control parameters on the microgrid stability.

D. Microgrid Oscillators-Based Model

Models expressed as so-called Kuramoto oscillators have been investigated in the literature for the analysis of the microgrid synchronization problem [31]. In the following it is shown that these models can be obtained from the reduced order models presented above by applying once again the singular perturbations technique. Consider the model (26)-(27) and assume that the time-constants L_a/R_a and L_b/R_b are sufficiently small too. By setting L_k/R_k to zero for $k=a,b$ and by indicating with y_k^{dq}, y_{ok}^{dq} and δ_y the variables of the reduced order model corresponding to z_k^{dq}, z_{ok}^{dq} and δ_z, respectively, from (26) and (27a) it follows

$$y_{ok}^{\mathrm{dq}} = y_k^{\mathrm{dq}} + \frac{1}{R_c}\Gamma_k(\delta_y)\left(I+\frac{X_c}{R_c}\Omega\right)^{-1} \cdot \sum_{j=a,b}\Gamma_j(\delta_y)^{-1}\bar{U}_j\begin{pmatrix}1\\0\end{pmatrix}, \quad k=a,b, \tag{30a}$$

$$0 = -\left(I+\frac{X_k}{R_k}\Omega\right)y_k^{\mathrm{dq}} + \frac{\bar{U}_k}{R_k}\begin{pmatrix}1\\0\end{pmatrix}, \qquad k=a,b, \tag{30b}$$

and from (27b)

$$\frac{d}{dt}\delta_y = m_a\bar{P}_a - m_b\bar{P}_b - m_a\bar{U}_a y_{oa}^d + m_b\bar{U}_b y_{ob}^d. \tag{31}$$

By computing y_k^{dq} from (30b) and by substituting in (30a), after some simple algebraic manipulations, one can write

$$y_{oa}^d = \rho_a - \rho_1\bar{U}_b\cos\delta_y + \rho_2\bar{U}_b\sin\delta_y, \tag{32a}$$

$$y_{ob}^d = \rho_b - \rho_1\bar{U}_a\cos\delta_y - \rho_2\bar{U}_a\sin\delta_y, \tag{32b}$$

TABLE I
CONTROL, LOADS AND TIE-LINE PARAMETERS

Parameters		Values	
		Dominant Loads	Dominant Line
Controls	m_a	$5\cdot10^{-4}$ rad/sW	$5\cdot10^{-4}$ rad/sW
	n_a	$5\cdot10^{-4}$ V/VAr	$5\cdot10^{-4}$ V/VAr
	$\bar{P}_a$	58 W	168 W
	$\bar{Q}_a$	2.6 kVAr	10 VAr
	$\bar{U}_a$	127 V	120 V
	m_b	$5\cdot10^{-4}$ rad/sW	$5\cdot10^{-4}$ rad/sW
	n_b	$5\cdot10^{-4}$ V/VAr	$5\cdot10^{-4}$ V/VAr
	$\bar{P}_b$	25 W	200 W
	$\bar{Q}_b$	1.3 kVAr	20 VAr
	$\bar{U}_b$	130 V	120 V
	ω	$2\pi60$ rad/s	$2\pi50$ rad/s
Resistences and inductances	R_a	0.13Ω	57Ω
	L_a	16mH	1.8mH
	R_b	0.25Ω	115Ω
	L_b	35mH	1.8mH
	R_c	0.5Ω	1.9Ω
	L_c	8mH	6.1mH

with

$$\rho_k = \frac{\bar{U}_k R_k}{R_k^2+X_k^2} + \frac{\bar{U}_k R_c}{R_c^2+X_c^2}, \qquad k=a,b, \tag{33a}$$

$$\rho_1 = \frac{R_c}{R_c^2+X_c^2}, \tag{33b}$$

$$\rho_2 = \frac{X_c}{R_c^2+X_c^2}. \tag{33c}$$

By substituting (32) in (31) it follows

$$\frac{d}{dt}\delta_y = \rho_3 + \rho_1\bar{U}_a\bar{U}_b(m_a-m_b)\cos\delta_y - \rho_2\bar{U}_a\bar{U}_b(m_a+m_b)\sin\delta_y, \tag{34}$$

where

$$\rho_3 = m_a\bar{P}_a - m_b\bar{P}_b - m_a\bar{U}_a\rho_a + m_b\bar{U}_b\rho_b. \tag{35}$$

The dynamic model (34) is representative of a Kuramoto oscillator and can be also derived by applying similar considerations to (28)-(29). The stability of the equilibrium points of (34) can be analytically investigated. In particular, by indicating with δ_y^{eq} an equilibrium point of (34) by taking the derivative of (34) at steady state with respect to δ_y^{eq} and by substituting in (33b) and (33c), a sufficient condition for local stability is

$$(m_a-m_b)R_c\sin\delta_y^{\mathrm{eq}} + (m_a+m_b)X_c\cos\delta_y^{\mathrm{eq}} > 0. \tag{36}$$

For typical microgrids and droop control parameters, the condition (36) is satisfied which means that the oscillator model predicts that the droop controlled microgrid is stable.

IV. STABILITY NUMERICAL ANALYSIS

In this Section a numerical analysis is carried out in order to validate the model order reductions in terms of the corresponding dynamic behaviors and stability properties.

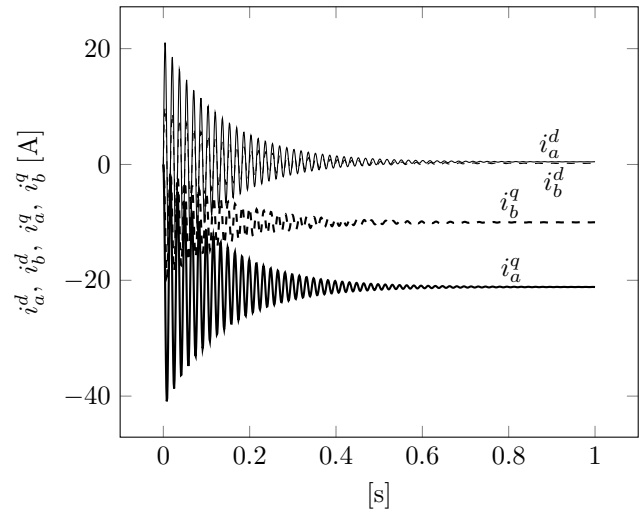

Fig. 2. Time domain evolutions of the loads currents for zero initial conditions and $m_a = 5 \cdot 10^{-4}$.

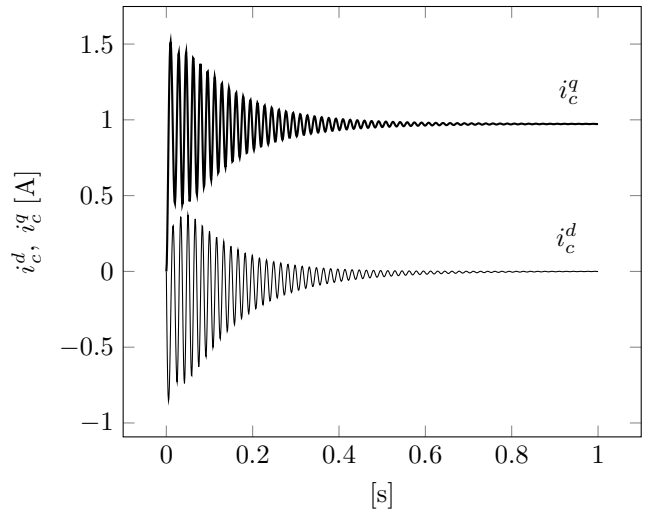

Fig. 3. Time domain evolutions of the tie-line currents for zero initial conditions and $m_a = 5 \cdot 10^{-4}$.

A. Microgrids with Dominant Loads

The equilibrium point of the model (16)-(17) with parameters indicated in the first column of Table I is $i_a^{d,\mathrm{eq}} = 0.46$ A, $i_b^{d,\mathrm{eq}} = 0.19$ A, $i_a^{q,\mathrm{eq}} = -21.16$ A, $i_b^{q,\mathrm{eq}} = -9.99$ A, $i_c^{d,\mathrm{eq}} = 0.8 \cdot 10^{-3}$ A, $i_c^{q,\mathrm{eq}} = 0.97$ A, $\delta^{\mathrm{eq}} = 3.7 \cdot 10^{-3}$ rad and the eigenvalues of the Jacobian computed around such equilibrium point are

$$\lambda_{1,2} = -59.95 \pm \jmath 384.37, \tag{37a}$$
$$\lambda_{3,4} = -7.63 \pm \jmath 379, \tag{37b}$$
$$\lambda_{5,6} = -6.98 \pm \jmath 377.96, \tag{37c}$$
$$\lambda_7 = -5.38, \tag{37d}$$

which show that the system is locally stable. Fig. 2 and Fig. 3 show the time domain evolutions of the currents. Fig. 3 particularly shows the presence of fast and slow modes in the tie-line currents dynamics. The time evolutions of the active and reactive powers present similar dynamics to those

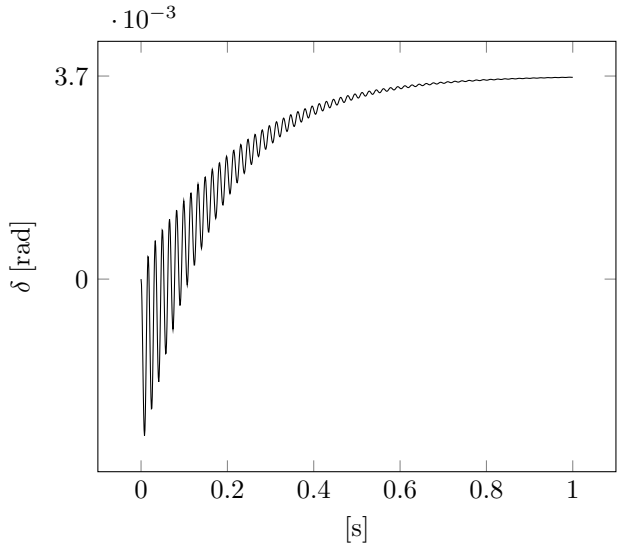

Fig. 4. Time domain evolution of the angle difference δ for zero initial conditions and $m_a = 5 \cdot 10^{-4}$.

represented in Fig. 3. Fig. 4 shows the time domain evolution of the angle $\delta = \theta_a - \theta_b$. In order to provide for the required active and reactive powers according to the corresponding reference values, at steady-state a non-zero angle difference is needed.

Fig. 5 shows the eigenlocus of (16)-(17) (triangles) and that of the reduced order model (20)-(21) (squares) by increasing m_a from the nominal value. Larger values of m_k are typically desired in order to obtain a better regulation of the active power, see (10a). For $m_a \geq 5 \cdot 10^{-3}$ some of the eigenvalues of (16)-(17) become positive real and the system is unstable. Fig. 5 shows also that the reduced order model predicts the instability occurring for a similar value of the frequency control parameter, since some eigenvalues become positive real for $m_a \geq 6.2 \cdot 10^{-3}$. Fig. 6 allows to verify that the error between the solutions of the seventh order model and those of the fifth order model is acceptable also for large signals. Moreover, Fig. 7 shows that also by increasing m_a the eigenvalue of (34), the real eigenvalue of (16)-(17) and the real eigenvalue of (20)-(21) are very close.

B. Microgrids with Dominant Tie-Line

The equilibrium point of the model (16)-(17) with parameters defined in the second column of Table I is $i_a^{d,\mathrm{eq}} = 2.11$ A, $i_b^{d,\mathrm{eq}} = 1.04$ A, $i_a^{q,\mathrm{eq}} = -0.02$ A, $i_b^{q,\mathrm{eq}} = -0.005$ A, $i_c^{d,\mathrm{eq}} = -0.66$ A, $i_c^{q,\mathrm{eq}} = -0.62$ A, $\delta^{\mathrm{eq}} = -0.02$ rad and the eigenvalues of the Jacobian computed around such equilibrium point are

$$\lambda_{1,2} = -63888.9 \pm \jmath 330.381, \tag{38a}$$
$$\lambda_{3,4} = -31666.7 \pm \jmath 330.327, \tag{38b}$$
$$\lambda_{5,6} = -309.497 \pm \jmath 321.959, \tag{38c}$$
$$\lambda_7 = -3.95662, \tag{38d}$$

which show that the system is locally stable. Fig. 8 and Fig. 9 show the time domain evolutions of the currents. Fig. 9

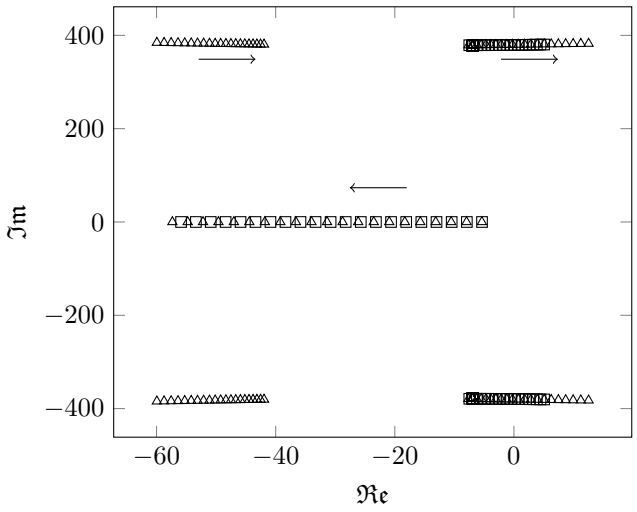

Fig. 5. Zoom of the eigenlocus of the model (16)-(17) (triangles) and eigelocus of the reduced order model (20)-(21) (squares), linearized around the corresponding equilibrium points for $m_a \in [5 \cdot 10^{-4}, 1 \cdot 10^{-2}]$. The arrows indicate increasing values of m_a. Complex conjugate eigenvalues become positive real for $m_a \geq 5 \cdot 10^{-3}$ and $m_a \geq 6.2 \cdot 10^{-3}$, respectively.

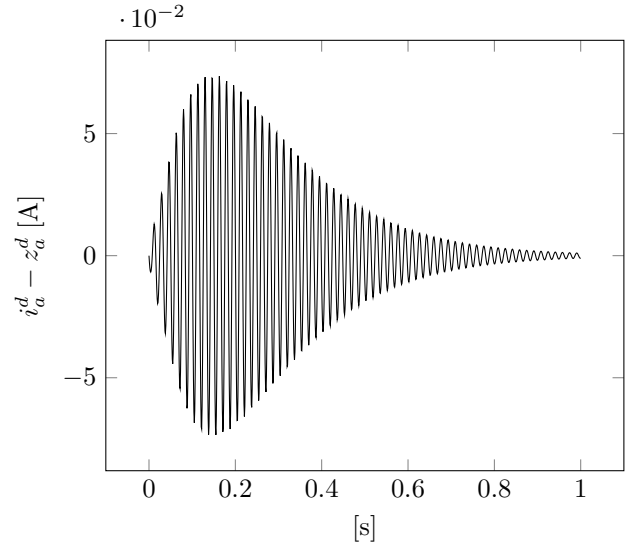

Fig. 6. Time evolution of the error between components of the load current i_a^d of (16)-(17) and that the reduced order model (20)-(21).

particularly shows the presence of slow modes in the tie-line currents dynamics. The time evolutions of the active and reactive powers present similar dynamics to those represented in Fig. 9. Fig. 10 shows the time domain evolution of the angle $\delta = \theta_a - \theta_b$.

Fig. 11 shows a zoom of the eigenlocus of (16)-(17) and the eigenlocus of the reduced order model (28)-(29) by increasing m_a from the nominal value. For $m_a \geq 15.36 \cdot 10^{-2}$ some of the eigenvalues of the linearized models from (16)-(17) become positive real which implies that the closed loop system is unstable. Fig. 11 shows also that the third order model (28)-(29) is able to detect the frequency droop control parameter value for which the seventh order model becomes unstable.

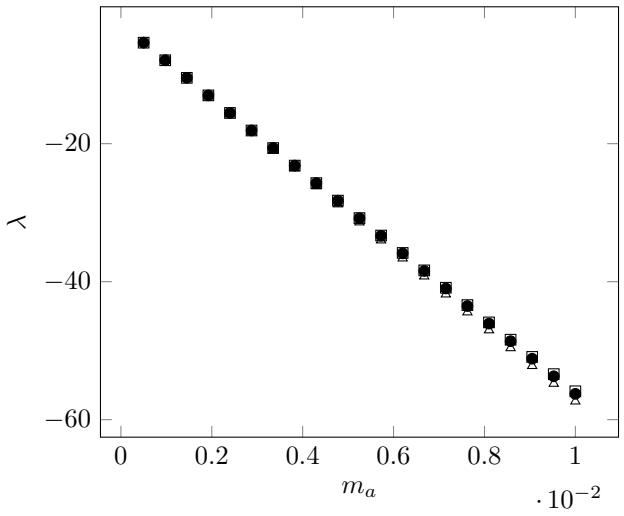

Fig. 7. Comparison between the eigenvalue of (34) (circles) and the real eigenvalue of (16)-(17) (triangles) and (20)-(21) (squares) versus $m_a \in [5 \cdot 10^{-4}, 1 \cdot 10^{-2}]$.

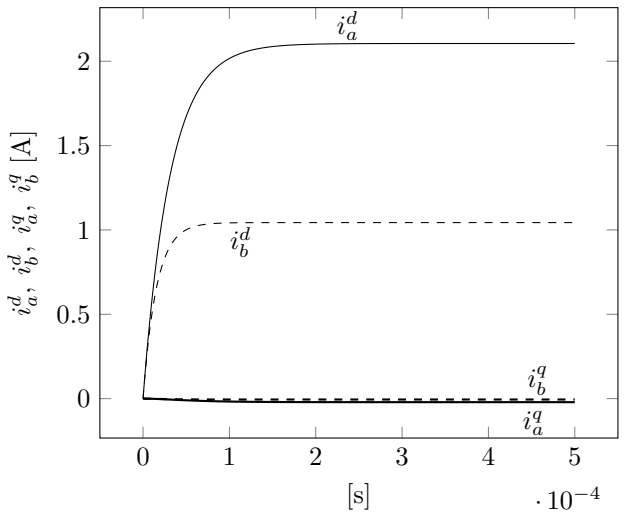

Fig. 8. Time domain evolutions of the loads currents for zero initial conditions and $m_a = 5 \cdot 10^{-4}$.

V. Experimental Results

In this Section experiments validating the microgrid stability analysis are presented. The results have been extracted from the intelligent Microgrid lab from Aalborg University, Denmark [37]. The experimental setup can be represented with the quivalent circuit in Fig. 1 where each ideal voltage supply is replaced by a real inverter with corresponding controllers and output filters whose equivalent scheme is shown in Fig. 12. Two three-phase three-legs Danfoss FC 302 inverters along with their corresponding output LC filters are adopted. The inverters are provided with inner voltages and currents control loops which are responsible for their proper operations and references tracking. The controllers are implemented by means of a dSPACE 1006 system. The same Matlab/Simulink schemes used for the control parts in the numerical simulations have been compiled to the dSPACE which has been responsible for the inverters control and the

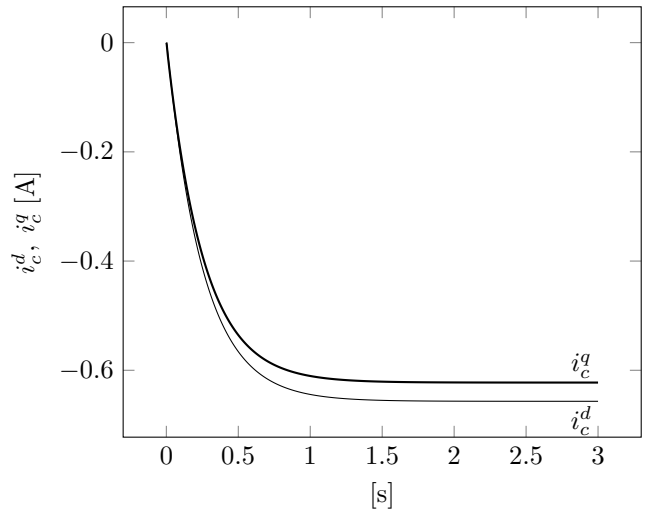

Fig. 9. Time domain evolutions of the tie-line currents for zero initial conditions and $m_a = 5 \cdot 10^{-4}$. Note the different time scale with respect to Fig. 8.

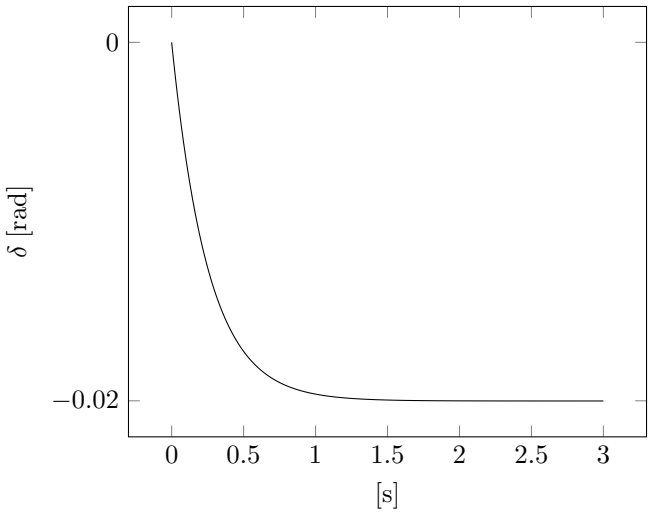

Fig. 10. Time domain evolution of the angle difference δ for zero initial conditions and $m_a = 5 \cdot 10^{-4}$.

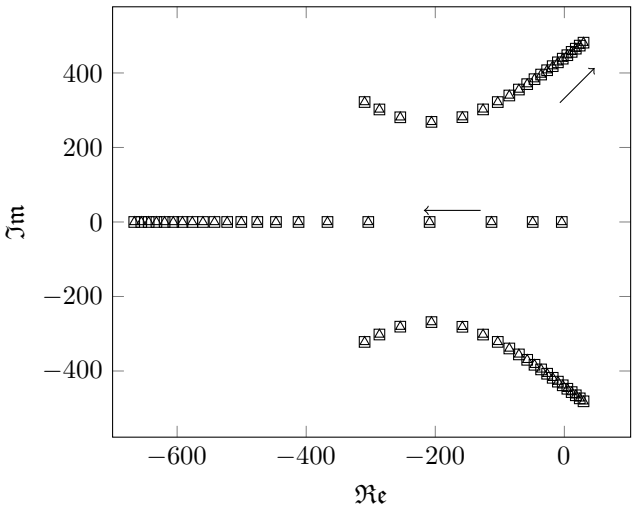

Fig. 11. Zoom of the eigenlocus of the model (16)-(17) (triangles) and eigenlocus of the reduced order model (28)-(29) (squares), linearized around the corresponding equilibrium points for $m_a \in [5 \cdot 10^{-4}, 20 \cdot 10^{-2}]$. The arrows indicate increasing values of m_a. Complex conjugate eigenvalues of both models become positive real for $m_a \geq 15.36 \cdot 10^{-2}$.

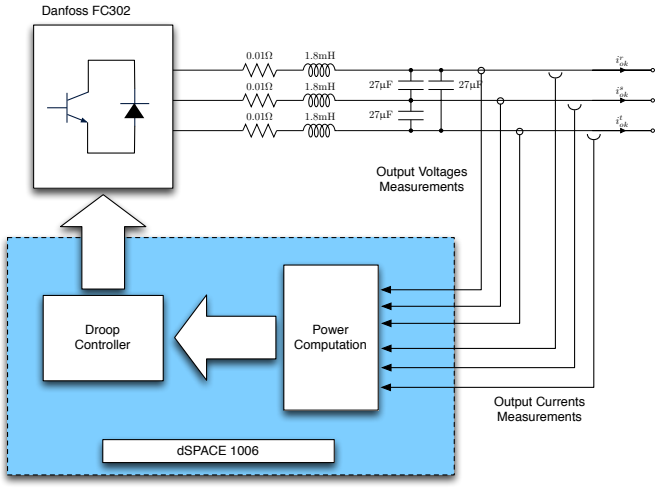

Fig. 12. Equivalent circuit corresponding to each inverter in the experimental setup.

data acquisition. The sampling time has been set to 100 μs.

In Fig. 13 it is shown the cabinet hosting the two inverters, the dSPACE system, a three-phase variable resistive-inductive bipole on the top and two three-phase variable resistors along its sides. The inverters output filters, the local loads and the line inductors are placed in the rear part of the cabinet. A DC voltage supply REGATRON TopCon TC.GSS with 650 V and a maximum current limited to 10 A is adopted.

The connections among each microgrid element, namely the two inverters, their corresponding local loads and the tie-line have been operated by means of three contactors. Further, three measurement boards with corresponding LEM sensors have allowed to measure all the relevant currents and voltages while the active and reactive powers and the angle difference have been computed by the dSPACE platform.

The experimental setup consits of a microgrid with dominant tie-line time-constant. The parameters of the setup are indicated in the second column of Table I. The first scenario considered consists of the microgrid completely formed, i.e., the two inverters are both connected through the tie-line. Fig. 14 shows the angle difference time evolutions, for different values of m_a, when, starting from the steady state, the angle of the inverter b is perturbed with an additive step disturbance of 0.1 rad. As the frequency droop control parameter is increased, the dynamic response becomes faster. Fig. 15 shows the currents of the load of the inverter b when the corresponding angle is perturbed. The disturbance effect on the load currents is negligible. The values of the three-phase currents i_b^{rst} are consistent with the steady state of the corresponding numerical simulations presented in the previous Section, see Fig. 8.

The second scenario considers the behavior at the connection of the inverters forming the microgrid. Fig. 16

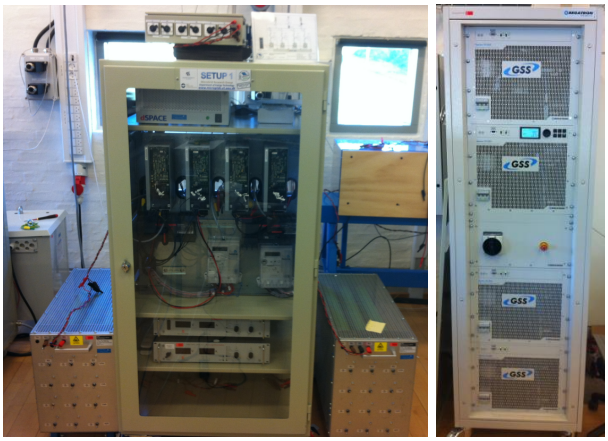

Fig. 13. Pictures of the experimental setup.

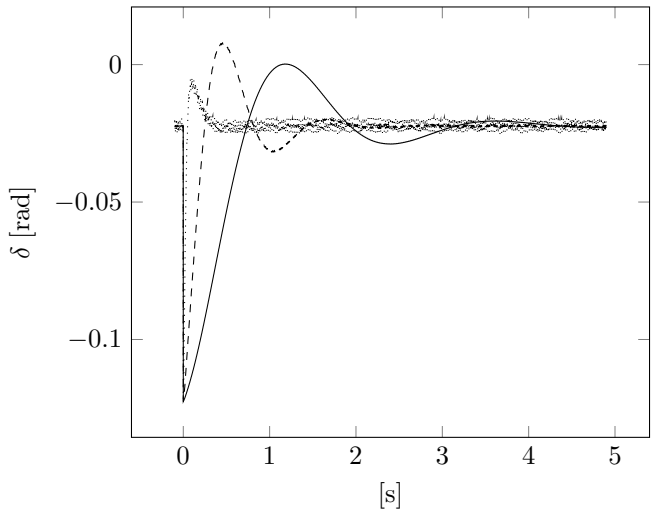

Fig. 14. Experiments. Time evolutions of the angle difference δ, for $m_a = 5 \cdot 10^{-4}$ (solid line), $m_a = 5 \cdot 10^{-3}$ (dashed line) and $m_a = 5 \cdot 10^{-2}$ (dotted line) when the angle of the inverter b is subject to an additive step disturbance of 0.1 rad.

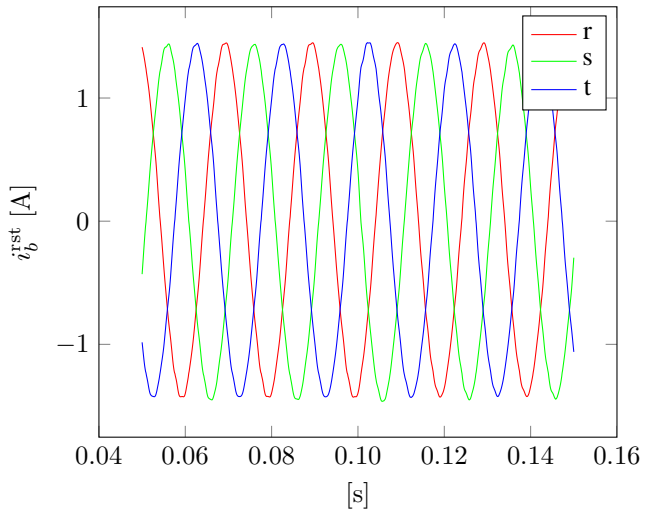

Fig. 15. Experiments. Time evoultions of the load currents i_b^{rst} for $m_a = 5 \cdot 10^{-4}$ when the angle of the inverter b is perturbed with an additive step disturbance of 0.1 rad at 0.1 s.

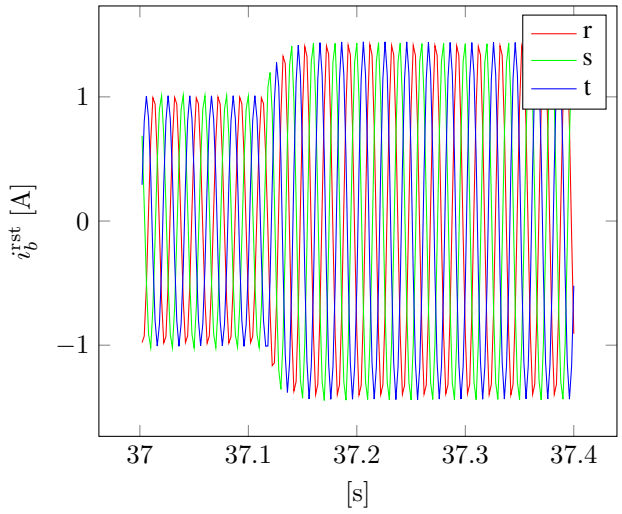

Fig. 16. Experiments. Time evoultions of the load currents i_b^{rst} for $m_a = 5 \cdot 10^{-4}$ when the inverters connect through the tie-line.

shows the currents of the load of the inverter b starting from the inverters in stand-alone operating conditions when the microgrid is formed. The formation of the microgrid changes the equilibrium point with respect to the case of independent inverters with corresponding local loads. The final steady state in Fig. 16 is the same as the one in Fig. 15.

The third scenario aims at highlighting the microgrid instability. Fig. 17 depicts the experimental results of the angle difference δ when the frequency droop control parameter m_a is subject to a step variation. The experiments show the instability for $m_a = 25.3 \cdot 10^{-2}$. For this value also the reduced order model predicts the instability so as shown by the numerical results in the previous Section.

VI. Conclusions

A systematic approach to model a microgrid with droop controlled inverters has been presented. By using a suitable state space transformation a closed loop model in explicit state space form has been derived. The time-scale separations between the line time-constant and the loads time-constants have been exploited by using singular perturbations and corresponding reduced order models have been obtained. Furthermore, by neglecting the currents dynamics a microgrid model in the form of Kuramoto oscillators has been derived. The models highlight the importance of the electrical dynamics and the influence of the frequency droop control parameters on the stability of the microgrid. Differently from the oscillators-based model, the singularly perturbed reduced order models are shown to predict the microgrid unstable behaviors, which are confirmed by the numerical and experimental results. The methodological steps applied to the simple microgrid topology considered in the paper can be adopted also for more complex networks for which the considered microgrid represent a basic subsystem. From a qualitative point of view one can conjecture that the currents dynamics influence the stability of the microgrid also for more complex

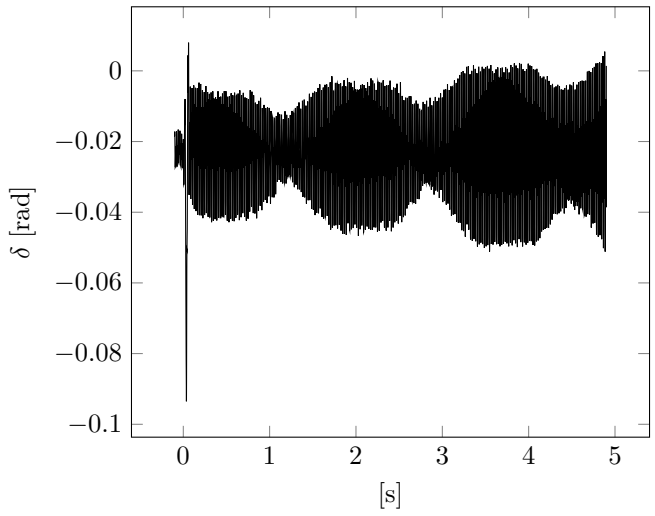

Fig. 17. Experiment. Time evolution of the angle difference δ for a step variation of m_a from $10 \cdot 10^{-2}$ to $25.3 \cdot 10^{-2}$.

topologies under large values of the droop control parameters. This is a possible direction for future research.

REFERENCES

[1] M. C. Chandorkar, D. M. Divan, and R. Adapa, "Control of Parallel Connected Inverters in Standalone AC Supply Systems," *IEEE Trans. on Industry Applications*, vol. 29, no. 1, pp. 136–143, 1993.

[2] J. M. Guerrero, M. Chandorkar, T.-L. Lee, and P. C. Loh, "Advanced Control Architectures for Intelligent Microgrids-Part I: Decentralized and Hierarchical Control," *IEEE Trans. on Industrial Electronics*, vol. 60, no. 4, pp. 1254–1262, 2013.

[3] Q.-C. Zhong, "Robust Droop Controller for Accurate Proportional Load Sharing Among Inverters Operated in Parallel," *IEEE Trans. on Industrial Electronics*, vol. 60, no. 4, pp. 1281–1290, 2013.

[4] Y. Mohamed and E. El-Saadany, "Adaptive Decentralized Droop Controller to Preserve Power Sharing Stability of Paralleled Inverters in Distributed Generation Microgrids," *IEEE Trans. on Power Electronics*, vol. 23, no. 6, pp. 2806–2816, 2008.

[5] W. Yao, M. Chen, J. Matas, J. M. Guerrero, and Z. M. Qian, "Design and Analysis of the Droop Control Method for Parallel Inverters Considering the Impact of the Complex Impedance on the Power Sharing," *IEEE Trans. on Industrial Electronics*, vol. 58, no. 2, pp. 576–588, 2011.

[6] J. M. Guerrero, J. Matas, L. G. de Vicuña, M. Castilla, and J. Miret, "Decentralized Control for Parallel Operation of Distributed Generation Inverters Using Resistive Output Impedance," *IEEE Trans. on Industrial Electronics*, vol. 54, no. 2, pp. 994–1004, 2007.

[7] A. Kahrobaeian and Y. A.-R. I. Mohamed, "Analysis and Mitigation of Low-Frequency Instabilities in Autonomous Medium-Voltage Converter-Based Microgrids With Dynamic Loads," *IEEE Trans. on Industrial Electronics*, vol. 61, no. 4, pp. 1643–1658, 2014.

[8] N. Bottrell, M. Prodanovic, and T. C. Green, "Dynamic Stability of a Microgrid with an Active Load," *IEEE Trans. on Power Electronics*, vol. 28, no. 11, pp. 5107–5119, 2013.

[9] U. Borup, F. Blaabjerg, and P. N. Enjeti, "Sharing of Nonlinear Load in Parallel-Connected Three-Phase Converters," *IEEE Trans. on Industry Applications*, vol. 37, no. 6, pp. 1817–1823, 2001.

[10] M. Savaghebi, A. Jalilian, J. C. Vásquez, and J. M. Guerrero, "Autonomous Voltage Unbalance Compensation in an Islanded Droop-Controlled Microgrid," *IEEE Trans. on Industrial Electronics*, vol. 60, no. 4, pp. 1390–1402, 2013.

[11] ——, "Secondary Control Scheme for Voltage Unbalance Compensation in an Islanded Droop-Controlled Microgrid," *IEEE Trans. on Smart Grid*, vol. 3, no. 2, pp. 797–807, 2012.

[12] D. De and V. Ramanarayanan, "Decentralized Parallel Operation of Inverters Sharing Unbalanced and Nonlinear Loads," *IEEE Trans. on Power Electronics*, vol. 25, no. 12, pp. 3015–3025, 2010.

[13] J. Kim, J. Guerrero, P. Rodriguez, R. Teodorescu, and N. Kwanghee, "Mode Adaptive Droop Control With Virtual Output Impedances for an Inverter-Based Flexible AC Microgrid," *IEEE Trans. on Power Electronics*, vol. 26, no. 3, pp. 689–701, 2011.

[14] Y. A.-R. I. Mohamed and A. A. Radwan, "Hierarchical Control System for Robust Microgrid Operation and Seamless Mode Transfer in Active Distribution Systems," *IEEE Trans. on Smart Grid*, vol. 2, no. 2, pp. 352–362, 2011.

[15] J. C. Vásquez, J. M. Guerrero, A. Luna, P. Rodriguez, and R. Teodorescu, "Adaptive Droop Control Applied to Voltage-Source Inverters Operating in Grid-Connected and Islanded Modes," *IEEE Trans. on Industrial Electronics*, vol. 56, no. 10, pp. 4088–4096, 2009.

[16] J. M. Guerrero, J. C. Vásquez, J. Matas, M. Castilla, and L. G. de Vicuña, "Control Strategy for Flexible Microgrid Based on Parallel Line-Inductive UPS Systems," *IEEE Trans. on Industrial Electronics*, vol. 56, no. 3, pp. 726–736, 2009.

[17] J. M. Guerrero, L. G. de Vicuña, J. Matas, M. Castilla, and J. Miret, "A Wireless Controller to Enhance Dynamic Performance of Parallel Inverters in Distibuted Generation Systems," *IEEE Trans. on Power Electronics*, vol. 19, no. 5, pp. 1205–1213, 2004.

[18] J. Matas, M. Castilla, L. G. de Vicuña, J. Miret, and J. C. Vásquez, "Virtual Impedance Loop for Droop-Controlled Single-Phase Parallel Inverters Using a Second-Order General-Integrator Scheme," *IEEE Trans. on Power Electronics*, vol. 25, no. 12, pp. 2993–3002, 2010.

[19] J. M. Guerrero, L. G. de Vicuña, M. Castilla, and J. Miret, "Output Impedance Design of Parallel-Conncted UPS Inverters With Wireless Load-Sharing Control," *IEEE Trans. on Industrial Electronics*, vol. 52, no. 4, pp. 1126–1135, 2005.

[20] J. M. Guerrero, J. C. Vásquez, J. Matas, L. G. de Vicuña, and M. Castilla, "Hierarchical Control of Droop-Controlled AC and DC Microgirds — A General Approach Toward Standardization," *IEEE Trans. on Industrial Electronics*, vol. 58, no. 1, pp. 156–172, 2011.

[21] S. M. Ashabani and Y. A.-R. I. Mohamed, "General Interface for Power Management of Micro-Grids Using Nonlinear Cooperative Droop Control," *IEEE Trans. on Power Systems*, vol. 28, no. 3, pp. 2929–2941, 2013.

[22] H. J. Avelar, W. A. Parreira, J. B. Vieira, L. C. G. de Freitasand, and E. A. A. Coelho, "A State Equation Model of a Single-Phase Grid-Connected Inverter Using a Droop Control Scheme With Extra Phase Shift Control Action," *IEEE Trans. on Industrial Electronics*, vol. 59, no. 3, pp. 1527–1537, 2012.

[23] E. A. A. Coelho, P. C. Cortizo, and P. F. D. Garcia, "Small-Signal Stability for Parallel-Connected Inverters in Stand-Alone AC Supply Systems," *IEEE Trans. on Industry Applications*, vol. 38, no. 2, pp. 533–542, 2002.

[24] L. Wang, X. Q. Guo, H. R. Gu, W. Y. Wu, and J. M. Guerrero, "Precise Modeling Based on Dynamic Phasors for Droop-Controlled Parallel-Connected Inverters," in *Proc. of the 21st International Symposium on Industrial Electronics*, Hangzhou, China, 2012, pp. 475–480.

[25] F. Gao, Z. Li, Y. Li, P. Wang, and H. Zhu, "Small-Signal Stability Analysis of Parallel-Connected Inverters Based on Time-Varying Phasor," in *Proc. of the 6th Conference on Industrial Electronics and Applications*, Beijing, China, June 2011, pp. 1239–1244.

[26] K. D. Brabandere, B. Bolsens, J. V. D. Keybus, J. Driesen, M. Prodanovic, and R. Belmans, "Small-Signal Stability of Grids With Distributed Low-Inertia Generators Taking Into Account Line Phasor Dynamics," in *Proc. of the 18th International Conference and Exhibition on Electricity Distribution*, Torino, Italy, June 2005, pp. 1–5.

[27] S. Tabatabaee, H. R. Karshenas, A. Bakhshai, and P. Jain, "Investigation of Droop Characteristics and X/R Ratio on Small-Signal Stability of Autonomous Microgrid," in *Proc. of the 2nd Power Electronics, Drive Systems and Technologies Conference*, Tehran, Iran, February 2011, pp. 223–228.

[28] S. V. Iyer, M. N. Belur, and M. C. Chandorkar, "A Generalized Computational Method to Determine Stability of a Multi-Inverter Microgrid," *IEEE Trans. on Power Electronics*, vol. 25, no. 9, pp. 2420–2432, 2010.

[29] V. Mariani and F. Vasca, "Stability Analysis of Droop Controlled Inverters via Dynamic Phasors and Contraction Theory," in *Proc. of the 12th European Control Conference*, Zurich, Switzerland, July 2013, pp. 1505–1510.

[30] ——, "Partial Contraction Analysis for Droop Controlled Inverters," in *Proc. of the 3rd International Conference on Systems and Control*, Algiers, Algeria, October 2013, pp. 287–292.

[31] J. W. S.-Porco, F. Dorfler, and F. Bullo, "Synchronization and

Power Sharing for Droop-Controlled Inverters in Islanded Microgrids," *Automatica*, vol. 49, no. 9, pp. 2603–2611, 2013.
[32] V. Mariani, F. Vasca, and J. M. Guerrero, "Dynamic-Phasor-Based Nonlinear Modelling of AC Islanded Microgrids Under Droop Control," in *Proc. of 11th International Multi-Conference on Systems, Signals and Devices*, Barcelona, Spain, February 2014, pp. 1–6.
[33] E. H. Allen and M. D. Ilic, "Interaction of Transmission Network and Load Phasor Dynamics in Electric Power Systems," *IEEE Trans. on Circuits and Systems*, vol. 47, no. 11, pp. 1613–1620, 2000.
[34] N. Pogaku, M. Prodanovic, and T. C. Green, "Modeling, Analysis and Testing of Autonomous Operation of an Inverter-Based Microgrid," *IEEE Trans. on Power Electronics*, vol. 22, no. 2, pp. 613–625, 2007.
[35] H. K. Khalil, *Nonlinear Systems*, 3rd ed. New Jersey: Prentice Hall, 2002.
[36] A. Engler and N. Soultanis, "Droop Control in LV-Grids," in *Proc. of the International Conference on Future Power Systems*, Amsterdam, The Netherlands, November 2005, pp. 1–6.
[37] Aalborg University, "Microgrid research programme," http://www.microgrids.et.aau.dk.

Valerio Mariani was born in 1979 in Firenze, Italy. He received the Ph.D. in Automatic Control in 2014 from the University of Sannio (Benevento, Italy) where he is now Assistant Researcher. He has been guest Ph.D. with the Microgrids Research Programme, Department of Energy Tehnology, Aalborg University. His research activity is focused on modeling techniques of microgrids with droop controlled inverters and on stability analysis of complex power systems with nonlinear techniques in general.

Francesco Vasca (M'94-SM'12) was born in 1967 in Giugliano (Napoli, Italy). In 1995 he received the Ph.D. in Automatic Control from the University of Napoli Federico II. Since 2000 he is Associate Professor of Automatic Control at the University of Sannio (Benevento, Italy). His research activity is focused on the analysis and control of switched systems (averaging, complementarity, dithering, real time hardware in the loop) with applications to power electronics, railway control and automotive control. Since 2008 he is Associate Editor for the IEEE Transactions on Control Systems Technology.

Juan C. Vásquez (M'12) received the B.S. degree in Electronics Engineering from Autonomous University of Manizales, Colombia in 2004 where he has been teaching courses on digital circuits, servo systems and flexible manufacturing systems. In 2009, He received his Ph.D degree in Automatic Control, Robotics and Computer Vision from the Technical University of Catalonia, Barcelona, Spain in 2009 at the Department of Automatic Control Systems and Computer Engineering, from Technical University of Catalonia, Barcelona (Spain), where he worked as Post-doc Assistant and also teaching courses based on renewable energy systems. Since 2011, he has been an Assistant Professor in microgrids at the Institute of Energy Technology, Aalborg University, Aalborg, Denmark, where he is the co-responsible of the microgrids research program. His current research interests include operation, power management, hierarchical control and optimization applied to Distributed Generation in AC/DC microgrids. He is currently member of the Technical Committee on Renewable Energy Systems TC-RES.

Josep M. Guerrero (S'01-M'04-SM'08) received the B.S. degree in telecommunications engineering, the M.S. degree in electronics engineering, and the Ph.D. degree in power electronics from the Technical University of Catalonia, Barcelona, in 1997, 2000 and 2003, respectively. Since 2011, he has been a Full Professor with the Department of Energy Technology, Aalborg University, Denmark, where he is responsible for the Microgrid Research Program. From 2012 he is a guest Professor at the Chinese Academy of Science and the Nanjing University of Aeronautics and Astronautics; and from 2014 he is chair Professor in Shandong University. His research interests is oriented to different microgrid aspects, including power electronics, distributed energy-storage systems, hierarchical and cooperative control, energy management systems, and optimization of microgrids and islanded minigrids. Prof. Guerrero is an Associate Editor for the IEEE TRANSACTIONS ON POWER ELECTRONICS, the IEEE TRANSACTIONS ON INDUSTRIAL ELECTRONICS, and the IEEE Industrial Electronics Magazine, and an Editor for the IEEE TRANSACTIONS on SMART GRID. He has been Guest Editor of the IEEE TRANSACTIONS ON POWER ELECTRONICS Special Issues: Power Electronics for Wind Energy Conversion and Power Electronics for Microgrids; the IEEE TRANSACTIONS ON INDUSTRIAL ELECTRONICS Special Sections: Uninterruptible Power Supplies systems, Renewable Energy Systems, Distributed Generation and Microgrids, and Industrial Applications and Implementation Issues of the Kalman Filter; and the IEEE TRANSACTIONS on SMART GRID Special Issue on Smart DC Distribution Systems. He was the chair of the Renewable Energy Systems Technical Committee of the IEEE Industrial Electronics Society. In 2014 he was awarded by Thomson Reuters as ISI Highly Cited Researcher.